SIMULATION OF THE UPWELLING THERMAL RADIATION SCATTERED BY AEROSOL, TAKING INTO ACCOUNT TEMPERATURE INHOMOGENEITIES ON A SURFACE PART 3. SMALL SCALE HIGH-TEMPERATURE ANOMALIES

S.V. Afonin, V.V. Belov, and I.Yu. Makushkina

Institute of Atmospheric Optics,
Siberian Branch of the Russian Academy of Sciences, Tomsk
Received October 18, 1996

We consider here some results of statistical simulation of thermal radiation distorted by aerosol in the spectral channel at 3.75 μm *at the presence of high-temperature small-size spatial anomaly on a homogeneous surface. The observations of small-size fire cells from space through the turbid atmosphere by means of the instrument with a medium spatial resolution have been simulated for different optical-geometrical situations. Investigations have been carried out in the frameworks of the theory of linear systems in the optics of disperse media.*

We also present data characterizing the distorting effect of different aerosols: continental and urban in the near-ground layer, as well as the post-volcanic layer in the stratosphere on measurement results. The analysis of calculational data has shown that aerosol factor can noticeably affect the accuracy of solution of the problem of early finding and estimation of the small-size fire cell from the satellite data in the case of high turbidity of the near-ground atmospheric layer.

1. INTRODUCTION

The results of simulation of the upwelling thermal radiation scattered by aerosol in the spectral channels of 3.75 and 10.8 μm for the case of large-scale temperature gradient on the underlying surface were considered in Ref. 2, as well as the situations were determined where the distorting effect of the gradients on the radiative temperature recorded by the instrument is more than 0.5 K due to the aerosol scattering. These results are based on the data on the pulse response of IR-channels (point spread function) obtained earlier[1] for different optical-geometrical conditions.

In this paper we study the effect of aerosol scattering on the intensity of upwelling thermal radiation for different type of temperature inhomogeneities, i.e., small-scale high-temperature anomalies. As in the previous case, the study is aimed at practical applications and is related with the problem on increasing the efficiency of the algorithms of aerospace detection and estimating the characteristics of the forest fires at the initial stage of their life. Thus, the term "small-size" refers to the situation when the size of high-temperature area is smaller than the element of the field of view of the radiometers of a medium spatial resolution.

It is necessary to note that serious attention in literature is paid to the study of different aspects of this problem, the creation of effective techniques and prompt algorithms of its solution.[3–6] There is also practical experience of using the satellite data for these purposes. The detailed overview of the modern state of the problem on early detection of the forest fires is presented in Ref. 3. The necessity of making atmospheric correction of the satellite data to achieve reliable solution of the problem is also considered here. However, the algorithms of atmospheric correction proposed for these purposes do not take into account the distorting effect of aerosol scattering. This paper presents some results that make it possible to quantitatively estimate possible effect of the size of the forest fire cells at the early stage of their development.

Let us make two comments in the conclusion of the introduction. It is known that the results of remote measurements in the spectral range of 3–5 μm serve as the main decoding parameter of the small-size fire cell. Because of this reason, we are limited by the study of the problem only for the channel at 3.75 μm. The second note is related to the technical problem on the existence of a "saturation threshold" for measuring in IR-channels, which is located in the range of 320–330 K for many instruments, in particular, for the AVHRR radiometer. In this paper we do not take into account this limitation, not considering it as a principle one. The example of solution of this technical problem is the MODIS instrument that has the IR channels with the saturation threshold of 400–500 K for detecting the fire cells.

0235-6880/97/02 114-05 $02.00

2. BASIC FEATURES OF THE SIMULATION

As earlier,[2] the calculation was performed of the intensity J_λ and radiative temperature T_λ of the natural radiation of the "atmosphere – underlying surface" system

$$J_\lambda = J^0_\lambda + J^{MS}_\lambda , \quad T_\lambda = B^{-1}_l [J_\lambda] ,$$

$$J^0_\lambda = J^0_{ATM} + J^0_{SURF} , \quad J^{MS}_\lambda = J^{MS}_{ATM} + J^{MS}_{SURF} ,$$

$$J^0_{SURF} (x', y') = B_\lambda [T_s (x', y')] \exp (- \tau),$$

$$J^{MS}_{SURF} (x', y') = = \iint_S h_\lambda(x - x', y - y') B_\lambda [T_s(x, y)] dx dy,$$

where J^0_{ATM}, J^0_{SURF}, J^{MS}_{ATM} and J^{MS}_{SURF} are the contributions of the atmosphere and the underlying surface into the intensity of direct (J^0_λ) and scattered (J^{MS}_λ) radiation, respectively, (x', y') are the coordinates inside the area S_0; τ is the optical thickness of the atmosphere; B_λ is the Plank function; B^{-1}_l is the inverse Plank function; T_s is the underlying surface temperature; $h_\lambda(x - x', y - y')$ is the point spread function; S is the effective spatial area of the adjacency effect formation. In our calculations S was limited by a circle with the center at the point of a cross of the optical axis of the receiver with the Earth's surface (x_0, y_0) and the radius R.

However, in the case under consideration it is necessary to take into account that the scale of inhomogeneities is comparable with the surface resolution S_0 of the receiver. So we have calculated the intensities of the direct $\bar{J}^0_{SURF}$ and scattered $\bar{J}^{MS}_{SURF}$ radiation averaged over the area S_0

$$\bar{J}^0_{SURF} = \frac{1}{S_0} \iint_{S_0} J^0_{SURF} (x', y') dx' dy',$$

$$\bar{J}^{MS}_{SURF} = \frac{1}{S_0} \iint_{S_0} J^{MS}_{SURF} (x', y') dx' dy'.$$

Assuming that the point spread function is invariant with respect to the shift in the limits of the field of view of the receiver, when calculating $\bar{J}^{MS}_{SURF}$ we used the function $h(x, y)$, the results of simulating of which and the description of its properties are given in Ref. 1.

3. OPTICAL-GEOMETRICAL CONDITIONS OF SIMULATION

As before, observations from satellites of NOAA series by means of IR channels of AVHRR radiometer were simulated in the numerical experiments:

spectral channel $\lambda = 3.75$ μm
zenith angle of observation $\Theta = 0$ and 45°
altitude of the observation platform 800 km
area of the element of spatial resolution of the instrument: $S_0 \approx 1$ km^2 at $\Theta = 0°$, and $S_0 \approx 4.0$ km^2 at $\Theta = 45°$.

Simulation was performed for the following optical and meteorological conditions of observations: cloudless atmosphere, molecular plus aerosol atmosphere; the atmosphere was also assumed to be spherically symmetrical, vertically stratified, horizontally homogeneous; for meteorological model of the atmosphere we took a midlatitude summer.

For aerosol models two situations were considered:

rural and urban aerosol in the near ground atmospheric layer up to 2 km (meteorological visual range S_m = 1, 2, 3, 5, 10, 20, 35 and 50 km) and the background aerosol in the troposphere and the stratosphere;

aerosol free atmosphere in the near-ground layer and the model of post volcanic stratospheric aerosol layer of the optical thickness from 0.015 (moderate load) to 0.15 (high load), which has the maximum extinction characteristics at the altitudes 15–20 km.

4. MODEL OF THE UNDERLYING SURFACE

The model of the underlying surface was set as follows. The element of the area S_0 was selected on the surface. The high-temperature part of the area $S_H < S_0$ with temperature T_H was taken to be at its center.

The value $S_H = L_H \times L_H$ (L_H is the linear size of the fire) varied in the limits from 10×10 to 1000×1000 m^2.

Fire temperature was taken $T_H = 600$ and 1000 K, that corresponded to the smouldering and combustion events. Temperature of the surrounding surface was $T_s = 294.2$ K.

5. RESULTS OF SIMULATION

Let us first consider the results of the study of the first event: turbid near-ground layer combined with the background aerosol in the troposphere and the stratosphere.

Figure 1 presents the data that give the qualitative and quantitative idea of the distorting effect of molecular and aerosol components of the atmosphere on the results of remote IR measurements at different values of the linear size L_H and temperature T_H of the fire. Comparison of the data for rural and urban aerosol, when the difference in the single scattering albedo reaches 1.8 times, makes it possible to separate out the role of scattering in the aerosol distortion of the value of the linear size of the high-temperature anomaly. Radiation temperature of the absolute black body (ABB) corresponding to the intensity of radiation $S_H B_\lambda(T_H) + (S_0 - S_H) B_\lambda(T_s)$ as a function of L_H is also shown here. As was expected, the analysis of the data obtained allows us to note, first of all, that the distortions from the molecular component under the midlatitude summer conditions dominate over others. It is just this the circumstance that explains the fact that the stage of atmospheric correction is limited, as a rule, by taking into account the molecular extinction only.[3] However, the distorting effect of aerosol becomes comparable with the molecular one, and it is necessary to take it into account under conditions of high atmospheric turbidity.

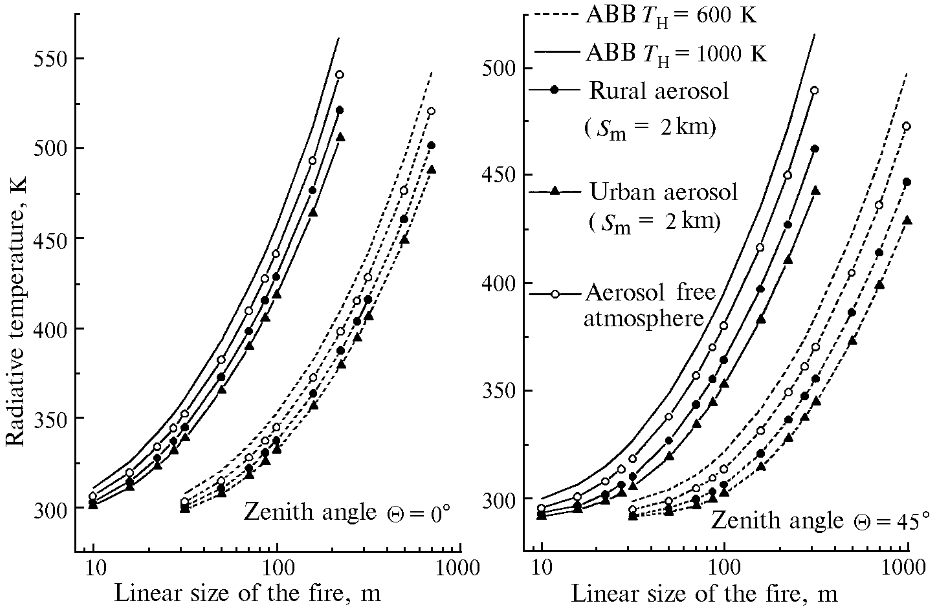

FIG. 1. Radiative temperature as a function of linear size of the fire.

The quantitative estimation of the possible aerosol effect on the accuracy of remote determination of the size L_H was performed using the following procedure:

a) the value $L^*_H(\tau_{aer})$, i.e. the observed fire size distorted by the aerosol-plus-molecular atmosphere, was "reconstructed" assuming a preset value of the radiative temperature T_λ based on the calculational data at different values of the aerosol optical thickness. Thus, the value $L^*_H(0)$ corresponds to the case of the molecular (aerosol free) atmosphere. The results of calculating L^*_H at T_λ = 315, 350 and 400 K are shown in Fig. 2 and demonstrate practically linear increase of the value L^*_H as τ_{aer} increases in the entire range of the radiative temperature considered. One also should note that the value T_λ = 315 K is often used as a threshold for finding the minimum detectable fire[3];

b) then the degree of the decrease of the observed fire size, which is caused by the neglect of the aerosol factor, was estimated based on the value $k_{aer} = L^*_H(\tau_{aer})/L^*_H(0)$. The results of calculations show that the relative variation of the coefficient k_{aer} as a function of τ_{aer} is quite accurately the same at different values L_H and T_H. Thus, the relative error in reconstructing the linear size of the high-temperature anomalies with the above discussed parameters depends only on τ_{aer}. The behavior of k_{aer} is shown in Fig. 3. If one neglects even the molecular extinction (i.e. no correction for the atmospheric effects is made at all), the coefficient k_{aer} decreases by the value by a factor of 0.80–0.85 that represents the degree of distorting the linear size due to the molecular component. This fact is also shown in Fig. 3.

Let us formulate the results of the study for the first situation.

a) Analysis of k_{aer} squared is indicative of the possibility of noticeable errors which result in underestimation (up to 1.5–2.5 times) of the fire area from the satellite data, if one neglects the distorting aerosol effect under conditions of high atmospheric turbidity.

b) It follows from the data at the value T_λ = 315 K that the linear size of the minimum detectable fire cell at the absence of aerosol is in the range of 15–50 and 30–100 m depending on the observation angle and temperature T_H. The increase of the atmospheric turbidity results in the increase of this value by 15–30% (Θ = 0°) and 25–50% (Θ = 45°).

c) Comparison of the data for rural and urban aerosols shows that for taking into account the distorting effect of aerosol it is necessary, to know τ_{aer}, the optical thickness of aerosol extinction. Then, the increase of the portion of scattering for the fixed value τ_{aer} from 50% (urban type) to 90% (rural type) results in the change of the value L^*_H by only about 5–10%.

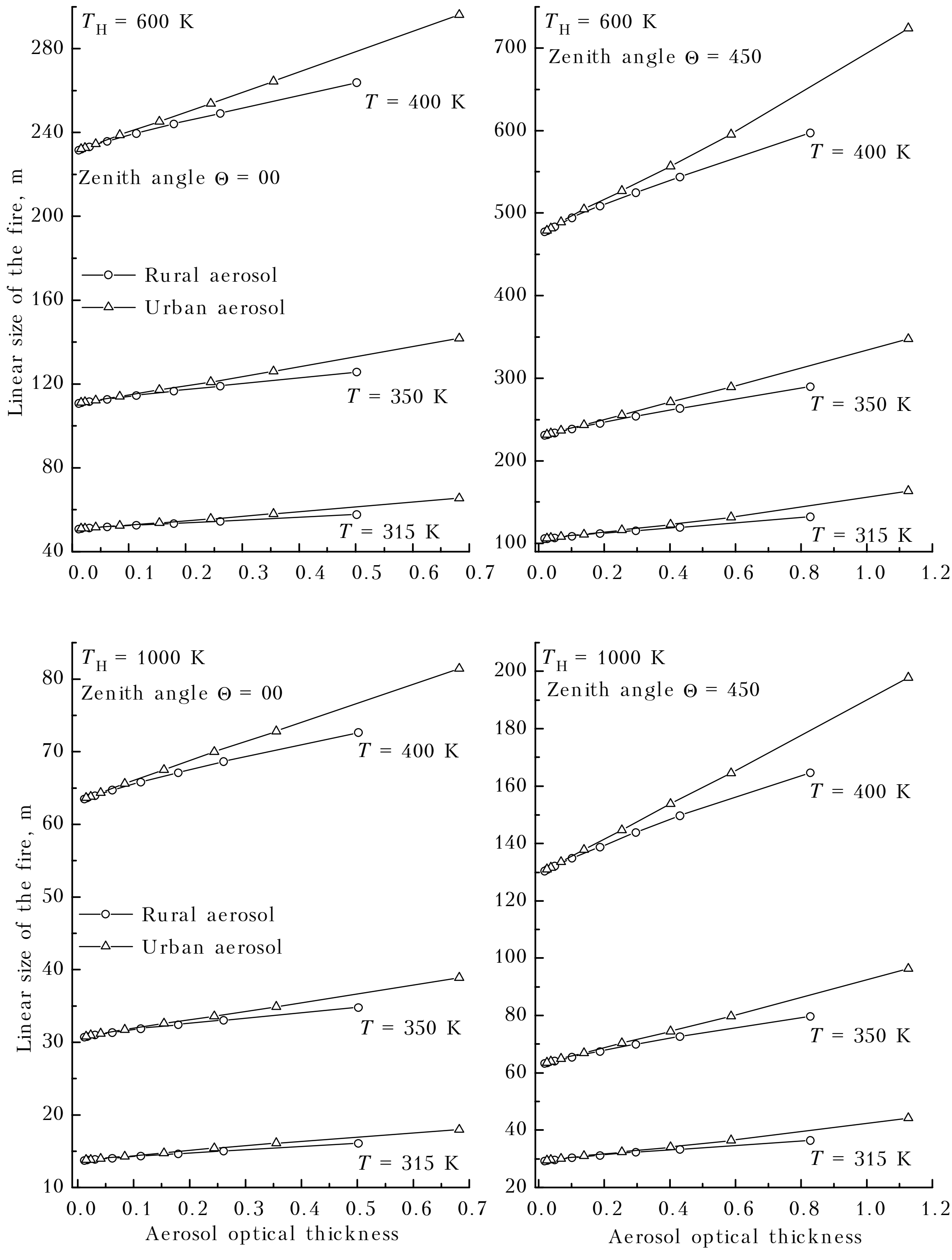

FIG. 2. Fire size as a function of the aerosol optical thickness.

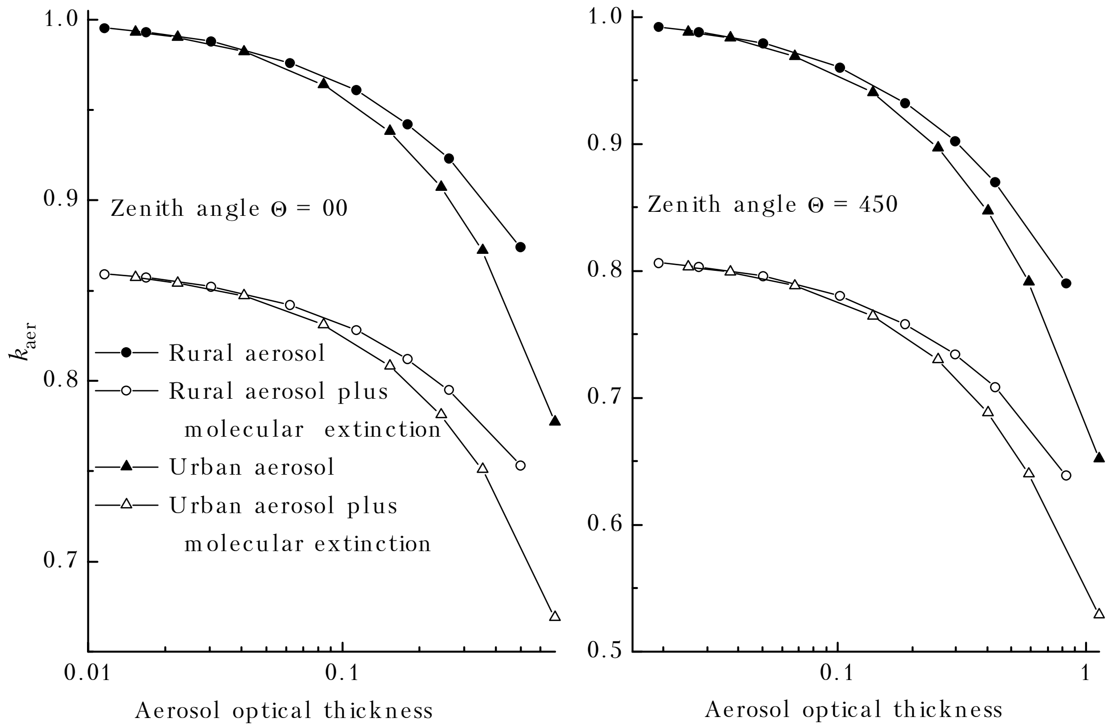

FIG. 3. The value k_{aer} as function of the aerosol optical thickness.

Let us now consider the results of the study for the second situation: there is an aerosol layer of the enchanced turbidity of the volcanic origin in the stratosphere. First of all, it is necessary to note that stratospheric aerosol has essentially less (in comparison with the near-ground one) distorting effect on the measured radiative temperature at the presence of the small-scale high-temperature anomalies. In this connection we do not show the illustrations and present only a brief list of the principal qualitative data obtained in the case of extremely high content of the volcanic aerosol in the stratosphere:

a) the error in remote estimations of the fire area does not exceed 30%;

b) the increase of the linear size of the minimum detectable fire is less than 6–12%.

Thus, under conditions of high turbidity of the near-ground atmospheric layer the distorting effect of aerosol can be a serious interference for the reliable solution of the problem on detecting small-scale high-temperature anomalies (fire cells) and determining their temperature and size based on the spaceborne IR data of a medium spatial resolution.

REFERENCES

1. S.V. Afonin, V.V. Belov, and I.Yu. Makushkina, Atmos. Oceanic Opt. **8**, No. 9, 756–762 (1995).
2. S.V. Afonin, V.V. Belov, and I.Yu. Makushkina, Atmos. Oceanic Opt. **8**, No. 12, 1013–1019 (1995).
3. Y. Kaufman and Ch. Justice, *Fire Products* (Version 1.2.2. Feb. 21, 1994, EOS ID#2741), MODIS ATBD, Fires March 10, 1994.
4. G.A. Zherebtsov, V.D. Kokourov, V.V. Koshelev, and N.P. Min'ko, Issled. Zemli iz Kosmosa, No. 5, 74–77 (1995).
5. T.V. Kondranin and E.V. Ovchinnikova, Issled. Zemli iz Kosmosa, No. 6, 51–57 (1995).
6. V.G. Astafurov and G.A. Titov, Atmos. Oceanic Opt. **9**, No. 5, 409–414 (1996).